Limnol. Oceanogr., 54(3), 2009, 735–745

Diurnal variations of surface seawater pCO_2 in contrasting coastal environments

Minhan Dai,[a,*] Zhongming Lu,[a,1] Weidong Zhai,[a] Baoshan Chen,[a] Zhimian Cao,[a] Kuanbo Zhou,[a] Wei-Jun Cai,[b] and Chen-Tung Arthur Chen[c]

[a] State Key Laboratory of Marine Environmental Science, Xiamen University, Xiamen, China
[b] Department of Marine Sciences, the University of Georgia, Athens, Georgia
[c] Institute of Marine Geology and Chemistry, National Sun Yat-sen University, Taiwan (China)

Abstract

We examined diurnal variations of surface seawater pCO_2 (partial pressure of CO_2) in a suite of coastal marine environmental systems in the vicinity of the South China Sea (SCS) from inshore and nearshore settings in Xiamen Bay, Shenhu Bay, and the southwestern Taiwan Strait, to offshore sites in the basin and on the slope of the northern South China Sea as well as in a coral reef system at Xisha Islands in the middle of the SCS. There were significant diurnal changes of surface pCO_2, ranging from 1.0 Pa to 1.6 Pa (10–16 μatm) in the offshore and oligotrophic sites, ~4.1 Pa in the Taiwan Strait, 5.1–15.2 Pa in Xiamen Bay and Shenhu Bay, to as high as 60.8 Pa in the coral reef system at Xisha Islands. Processes that modulate these pCO_2 diurnal variations were temperature, tide or current, and biological controls. Temperature was a major driver of the pCO_2 diurnal variability in the oligotrophic regions, while tidal effects were important in the nearshore. In the coral reef system, biological metabolism dominated variability. Diurnal variability could have a potentially important implication on the estimate of air–sea CO_2 fluxes, which may result in an uncertainty of $\pm$0.48–0.77 mmol C m^{-2} d^{-1} for the offshore sites in the SCS. Such uncertainties were larger in nearshore settings.

The constraint of air–sea CO_2 fluxes and their variability at various time and spatial levels remain a central task in global carbon and climate studies. Coastal ocean may represent one of the hot spots, which typically exerts poorly constrained and hotly debated air–sea CO_2 exchange rates (Cai and Dai 2004; Borges et al. 2005; Cai et al. 2006). The extreme heterogeneity and dynamic nature of coastal oceans may critically affect the reliability of reported CO_2 flux data. Moreover, CO_2 is also an important biogeochemical parameter that provides insights into biological production, calcification and potential hydrogen (pH) changes.

While it is clear that most of the oceanographic observations have involved shipboard operations on a seasonal timescale, growing evidence has suggested the importance of intra-seasonal variability to constrain oceanic changes (Bates et al. 1998; Fransson et al. 2004). Diurnal variability is one of these. Many physical and biogeochemical processes exert dynamic changes at a diurnal scale. These diurnal-scale processes include, but are not limited to, radiation forcing (Dickey 2004), tidal cycling, and temperature fluctuation to biological metabolism (Marra 1997). Knowledge of diurnal variations in physical, biological and chemical parameters is, thus, essential to our biogeochemical understanding of a specific system. Knowledge on the range of diurnal changes is also important in the determination of sampling strategy (Dickey and Bidigare 2005), given the fact that most shipboard sampling programs have not sampled frequently enough to characterize the daily cycle of many biogeochemical parameters such as phytoplankton productivity (Kinkade et al. 1999).

DeGrandpre et al. (2004) characterized pCO_2 variability in the eastern equatorial Pacific Ocean on hourly to weekly timescales in a 14-d Lagrangian drifter experiment during GasEx-2001. They found that the diurnal pCO_2 variability was dominated, in order of significance, by heating, net community metabolism, and dissolved inorganic carbon (DIC) depletion. Different from most continuous observations, this experiment was not conducted at a fixed station. Rather, samples were taken by following a drifter which traveled ~715 km during the experiment.

Biological turnover (represented by Apparent Oxygen Utilization) and mixing (represented by salinity) were found to be the two primary control factors of seawater pCO_2 during a 16-month study period in the surface water of the Baltic Sea (Kuss et al. 2006). During a Swedish–South African Expedition to the eastern Atlantic sector of the Southern Ocean (Fransson et al. 2004), it was found that fCO_2 and dissolved oxygen (DO) followed the diurnal cycle of biological production during high light intensity, and respiration during the night, at one of the three sites. However, two other sites they examined did not exhibit a clear trend of diurnal variations. On the other hand, the diurnal variation of pCO_2 was found to depend mainly on the tidal cycle during a 32-h continuous observation of pCO_2 variations in surface seawater along the Belgian coast (Borges and Frankignoulle 1999).

Some researchers also made observations of pCO_2 in coral ecosystems, and they found that the range of seawater pCO_2 and the diurnal pCO_2 amplitude were very large (7.4–108.3 Pa and 4.1–85.0 Pa, respectively; 1 Pa is equal to 9.869233 μatm) in some reef systems located at different reef sites around the world (Bates et al. 2001). This

* Corresponding author: (mdai@xmu.edu.cn).
[1] Present address: Department of Mathematics and the Atmospheric Marine and Coastal Environment Program, Hong Kong University of Science and Technology, Kowloon, Hong Kong, China

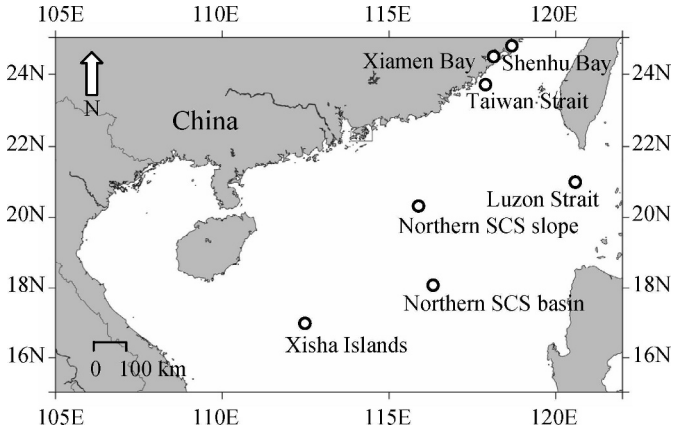

Fig. 1. Map of the South China Sea showing the experimental sites.

variability was mainly controlled by biological processes such as photosynthesis, respiration, and calcification or dissolution.

Recently, Yates et al. (2007) measured distinct diurnal variations of oxygen and the carbonate system in Tampa Bay and Florida Bay, with clear diurnal trends being shown in Tampa Bay for all measured parameters. These authors suggested that the diurnal variation in the carbonate system was dominated by primary production or respiration in Tampa Bay and calcium carbonate precipitation or dissolution in Florida Bay.

Despite the progress being made, studies on diurnal variations of the carbonate system in the coastal ocean are deficient in many areas and also limited. What is particularly lacking has been the comparison of diurnal changes in different coastal environmental settings, which may provide insights into the controls that modulate the diurnal variability. In this study, we selected a suite of coastal environmental settings to examine this important issue. What follows concentrates mainly on the patterns of surface seawater pCO_2 diurnal variations in different environmental settings and their control mechanisms, and to what extent the air–sea CO_2 flux would be affected is discussed taking into consideration these diurnal variations.

Methods

Study sites—Experiments were all conducted in the vicinity of the South China Sea (SCS), covering a variety of environmental settings spanning bays (Xiamen Bay and Shenhu Bay), the coastal shelf (Taiwan Strait), and offshore regions in the northern SCS. Also selected was a coral reef system in the SCS (Xisha Islands). These sites represent different geographical locations and hydrographic conditions. Climatic variations in the atmosphere at all these sites are dominated by the East Asian Monsoon. The locations of these sites are shown in Fig. 1 with detailed coordinates, and the experiment implementation time span is shown in Table 1. Also shown in Table 1 are the ranges of dissolved inorganic nitrogen (DIN) and chlorophyll *a* (Chl *a*) to better characterize the level of nutrients and potential biological activities at each site.

The SCS is one of the largest marginal seas with a deep semi-closed basin and wide continental shelves to the northwest and south. Its northern shelf, slope and the northern basin areas are fed by a major world river (the Pearl River) and potentially influenced by the West Pacific (the West Philippine Sea) via the Luzon Strait through the intrusion of Kuroshio branch water (Yuan et al. 2006; Fig. 1). Our northern SCS slope station (115°45′E, 20°11′N) was situated to the southwest of Dongsha Island on the shelf of the northern SCS with a water depth of ~1000 m. The northern SCS basin station (116°00′E, 18°00′N) had a water depth of ~3840 m, representing another open-area site of the oligotrophic SCS. Our observation site (120°30′E, 21°00′N) at the Luzon Strait had a water depth of ~1660 m. All these offshore sites are characterized by depleted nutrients in the surface layer and low levels of Chl *a* as shown in Table 1.

The Taiwan Strait is located at the confluence of the East China Sea and the SCS in the west Pacific. It is a shallow strait with ~60 m in average depth, and is ~180 km wide,

Table 1. Experimental sites and observation time. Also shown are the concentration ranges of DIN and Chl *a*, and the average tidal range at the observation sites. SCS = South China Sea.

Site	Coordinate	Experiment time span	DIN (μmol L^{-1})	Chl *a* (μg L^{-1})	Tidal range* (m)
N. SCS slope	115.76°E, 20.15°N	10 Jul 04–11 Jul 04	0.06±0.07†	0.12	0.2–0.4
N. SCS basin	116.00°E, 18.00°N	13 Jul 04–14 Jul 04	0.013±0.006†	0.09	0.4–1.2
Luzon Strait	120.50°E, 21.00°N	06 Jul 07–07 Jul 07	<0.05‡	0.05–0.1§	0.2–0.6
Taiwan Strait	117.85°E, 23.64°N	29 Jul 04–30 Jul 04	0.1–0.3	0.50–0.60	0.6–2.1
Xiamen Bay	118.06°E, 24.45°N	31 Jan 07–07 Feb 07	~18.7‖	0–4.0	2.1–4.5
Shenhu Bay	118.68°E, 24.67°N	17 Jun 05–24 Jun 05	>35¶	4.20–5.99#	2.8–5.6
Xisha Islands	112.33°E, 16.83°N	23 Jan 06–25 Feb 06	<0.3	0.19	0.2–1.8

* Difference between high tide and lower tide. Based on the tide height data of adjacent tide stations, from annual tide tables compiled by the National Marine Data and Information Service of China.
† According to Chen and Chen (2006).
‡ Based on Chen et al. (2003).
§ Based on Liu et al. (2002).
‖ According to Guo et al. (1998).
¶ According to the Marine Environmental Quality Report 2005 of the Quanzhou City (http://www.coi.gov.cn/hygb/dfhjzl/2005/qz2005/).
# Based on Luo (2002) and Ruan (2001).

350 km long. Waters of the South and East China Seas are exchanged through the strait (Jan et al. 2002). Circulation in the Taiwan Strait is complex. There is a northward current on the eastern side and a southward current on the western side. The source waters include the SCS water, Kuroshio branch water, and coastal waters including the Changjiang diluted water (Chen 2003). Currents in the Taiwan Strait are modulated by the annual cycle of monsoonal forcing but may be impeded by the complex bottom topography. Furthermore, the Taiwan Strait is well-known for its upwelling systems, the dynamics of which are still not fully understood (Jan et al. 2002).

Shenhu Bay is located on the central western coast of the Taiwan Strait (118°38′–118°41′E, 24°38′–24°40′N; Fig. 1). The mouth of the Bay is ~4.5 km wide. Shenhu Bay has a yearly average temperature of 20–21°C. Its average tidal range is 396 cm without major river inflow. The salinity variation was within 31–34 during our observation period. While the Shenhu Bay station is also located in the Taiwan Strait area, it is only a few kilometers away from the shore (Fig. 1). Consequently, tides may play a more important role.

Xiamen Bay is located at the lower reach of the Jiulong River estuary, on the west side of the Taiwan Strait (Fig. 1). Xiamen Bay has a regular semi-diurnal tide with a range very similar to Shenhu Bay (average ~396 cm), and the maximal tidal difference is 642 cm. The study site is located at 118°04′E, 24°27′N, ~100 m away from the shore, and had a salinity range of 25.4–27.5 during the experiment.

Xisha Islands (111°11′–112°54′E, 15°46′–17°08′N) are located in the NW SCS and characterized by coral reefs. The coral reefs sit on the Xisha continental slope at a water depth of ~1000 m, but are separated from the upper continental slope by the Zhongsha Trough, Xisha Trough and valleys with depths ranging from 1500 m to 2500 m. The seawater in the region is generally free from terrestrial substances and river plume influences (Nie et al. 1996), and thus is also characterized by low nutrients (Table 1). The climate of the Xisha area belongs to the tropical marine monsoon system with an annual average sea surface temperature (SST) of 27.2 ± 0.38°C. The surface seawater salinity is between 33.3 and 34.0 (Nie et al. 1996). Our experiment was conducted at Yongxing Island, which has a surface area of ~2 km^2 and is the largest of the Xisha Islands, and also of the SCS. The sampling point was located at the Yongxing reef flat, ~250 m away from the island shore. The water depth was ~5 m, and the water depth in the entire Yongxing reef flat ranges from <1 m to ~10 m.

p*CO_2 measurement*—Surface seawater was pumped from an intake at a depth of ~1 m for online measurements or sampling. pCO_2 in seawater was measured mainly using the so-called shower-head water–air equilibrator and a Non-Dispersive Infra-Red detector as previously described (Zhai et al. 2005). The system was calibrated every 3–12 h on the Xisha Islands and about every 24 h at other sites, in order to correct the instrument drift by using standard CO_2 gas (National Research Center for Certified Reference Materials, China) with an uncertainty of <1%.

pCO_2 in water and air were also measured using a homemade in situ fiber-optical chemical pCO_2 sensor deployed together with a mooring system for the experiments in Shenghu and Xiamen bays (Lu et al. 2008). The sensor is based on a gas-permeable liquid-core waveguide, and has a response time of <2 min (95% response) and an optimal precision of <0.1 Pa. During the observations at the Shenhu Bay, in addition to the pCO_2, salinity and temperature data were also recorded with moored sensors at a time interval of 3 h, and were transmitted to a land-based station instantaneously via satellite. In the Xiamen Bay diurnal observation experiment, pCO_2 sensor was deployed at a floating dock.

The air–sea CO_2 flux, 'F,' is generally estimated using: $F = k \times K_H \times \Delta pCO_2$, where k is the gas-transfer velocity of CO_2, which was calculated from wind speed based on the Wanninkhof (1992) equation. K_H is the solubility of CO_2 in seawater (Weiss 1974) and ΔpCO_2 is the sea–air pCO_2 difference. Note that the unit of K_H has been modified because of Pa units.

Measurements of other parameters—Salinity and temperature were measured using either a multiparameter sonde (YSI 6000UPG3-B-M-T, YSI 6600, YSI) or a SEACAT thermosalinograph system (CTD, SBE21; Sea-Bird). Dissolved oxygen was measured mainly using YSI or CTD or WTW's DO probe (CellOx 325; WTW). Winkler titration with a precision of 0.05 mg L^{-1} was also carried out for calibration. Total alkalinity (TA) was determined using an automated Gran titration analyzer with a precision of 0.1% (Cai et al. 2004). DIC was measured with a nondispersive infrared CO_2 analyzer with a precision of 0.1% (Cai et al. 2004). TA and DIC were calibrated against a certified reference material from A. Dickson's laboratory. pH was measured with an Orion pH glass electrode (ROSS Combination pH/model 81-02) and a Corning pH meter (Model pH/ion analyzer 350) with a precision of 0.005 pH units. We used three pH buffers (4.01, 7.00, and 10.01) certificated by National Institute of Standards and Technology for calibration. In addition to the discrete measurements, continuous measurements were also conducted for pH using the YSI sonde incorporated with a pH probe. Atmospheric temperature, wind speed, and air pressure were measured using a ship-board weather station (R. M. Young).

Evaluation of temperature and nontemperature effects on p*CO_2 variations*—To evaluate the relative importance of temperature and nontemperature effects on pCO_2 variations, we normalized aqueous pCO_2 to the average SST of the sea area under survey using Eq. 1 according to Takahashi et al. (2002):

$$N\,pCO_2 = (\text{in situ } pCO_2) \times \exp[0.0423\,(T_{ave} - T_{\text{in situ}})] \quad (1)$$

where N pCO_2 denotes temperature-normalized pCO_2. T is the temperature in °C, and the subscripts 'ave' and 'in situ' indicate the average and in situ values respectively.

Table 2. Summary of the range of diurnal seawater pCO_2, temperature (SST = sea surface temp), dissolved oxygen (DO), and mixed-layer depth (MLD) variations at the observation sites under study. SCS = South China Sea.

Sites	Water depth (m)	Diurnal range				
		pCO_2 (Pa)	SST (°C)	Salinity	DO (mg L^{-1})	MLD* (m)
N. SCS slope	~1000	37.5–38.5	29.1–29.9	34.13–34.20	6.27–6.33	44±5.7
N. SCS basin	>3000	39.6–41.2	30.1–31.4	34.19–34.32	6.15–6.25	43±8.6
Luzon Strait	~1660	40.4–42.0	30.4–31.6	33.62–33.78	6.04–6.18	18±1.6
Taiwan Strait	48	36.6–40.5	24.2–26.5	33.28–33.94	N/A	N/A
Xiamen Bay	2–6	47.6–57.8	14.5–15.2	25.40–27.50	N/A	N/A
Xisha Islands	3–5	18.7–94.2	20.2–28.2	33.70–34.30	4.18–10.19	N/A

* MLD is calculated according to the MLD threshold criterion of $\Delta\sigma_\theta = 0.125$ kg m^{-3} (Montegut et al. 2004).

Results

Table 2 summarizes the seawater pCO_2, temperature, and DO variation in our experimental sites. The amplitudes of the pCO_2 diurnal variation in our experiment sites were generally consistent with reports in similar environments. In the offshore region, the pCO_2 variation amplitude was 1.0–1.6 Pa, which is slightly higher than that in the Eastern equatorial Pacific Ocean (0.2–0.6 Pa; Degrandpre et al. 2004). The pCO_2 amplitudes reached 5.1–15.2 Pa in Xiamen Bay and Shenhu Bay, which is slightly lower than that in Tampa Bay or Florida Bay (14.2–22.3 Pa; Yates et al. 2007). In the Xisha coral reef ecosystem, the pCO_2 amplitudes were as high as 20.3–60.8 Pa, which is, however, similar to the pCO_2 amplitudes of 4.2–86.1 Pa in other coral reef systems (Bates et al. 2001).

Offshore sites—Figures 2–4 shows our diurnal observations for the seawater pCO_2 and relevant parameters during the July 2004 and July 2007 surveys at three offshore sites, on the SCS slope, in the SCS basin, and at the Luzon Strait (*see* Fig. 1 for the locations). pCO_2 at these sites had a peak-to-peak diurnal change of ~1.0 Pa on the slope, ~1.6 Pa in the basin and at the Luzon Strait (Figs. 2–4; Table 2). At the basin station (Fig. 3a), the in situ pCO_2 ranged from 39.7 Pa in the early morning to 41.3 Pa in the afternoon, apparently correlated with SST (Fig. 3b). As a comparison, the salinity remained nearly constant, with limited peak-to-peak changes of 0.1–0.2. The line-shape T – S diagram may further suggest that the surface seawater was mainly affected by mixing of two different water masses at the slope while the bulb-like T – S diagram at the basin station suggests that the water mass in this area was relatively homogeneous (Fig. 5). This is also reflected by the fact that the basin station has the largest in situ pCO_2 variation and smallest N pCO_2 variation among the three oceanic sites (Fig. 6). Slightly differently, pCO_2 at the Luzon Strait station showed a more complex diurnal variation with a relatively larger salinity variation range (Fig. 4a,b). This was also reflected by the T – S diagram (Fig. 5), where at least four mixing processes can be identified. As a consequence, no clear diurnal cycle of in situ pCO_2 was observable (Fig. 4) and N pCO_2 variation range was largest at this location (Fig. 6).

Nearshore settings—To study tide or current effects at nearshore settings, we conducted three fixed-station observations at different sites. The Taiwan Strait station was located ~35 km offshore on the shelf influenced by coastal upwelling. The two major water masses that controlled the physical and chemical properties of seawater were the surface water (characterized by high temperature but low salinity) and the bottom water (characterized by low temperature but high salinity). Although we do not intend to examine the dynamics of upwelling in any detail in this study, clearly, water masses were influenced by upwelling on a short timescale of 24 h along with the effect of tidal mixing (Fig. 7). Nevertheless, the surface seawater pCO_2 had a diurnal range of ~ 4.1 Pa, the change pattern of which was closely correlated with the water mass change featured by upwelling, as evidenced by the coherent variation between pCO_2 and salinity (Fig. 7). During the period when the mooring was deployed in the Shenhu Bay,

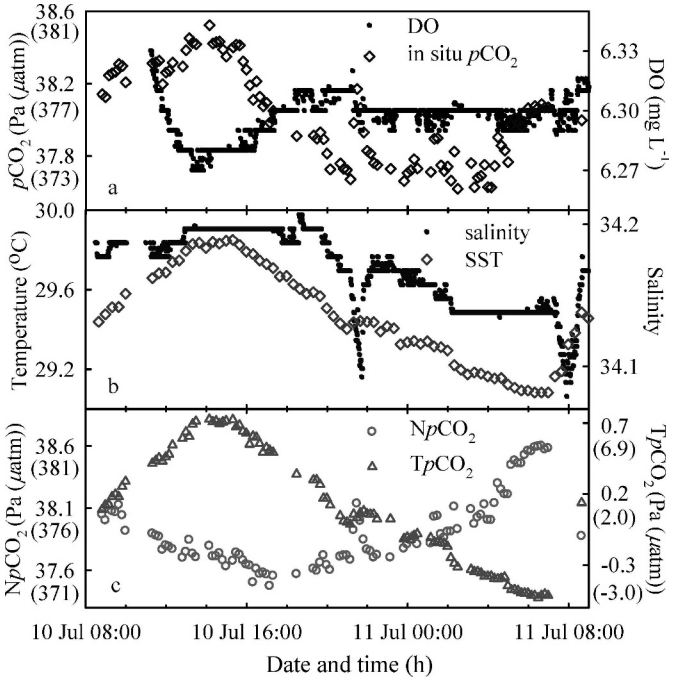

Fig. 2. Diurnal variations of surface seawater pCO_2, DO, temperature, and salinity at the slope of northern SCS (a, b). Also shown are the variations of temperature-normalized pCO_2 ($NpCO_2$) and $TpCO_2$ (pCO_2 offset caused by temperature variations, *see* text for details) (c). The figures were plotted by local time.

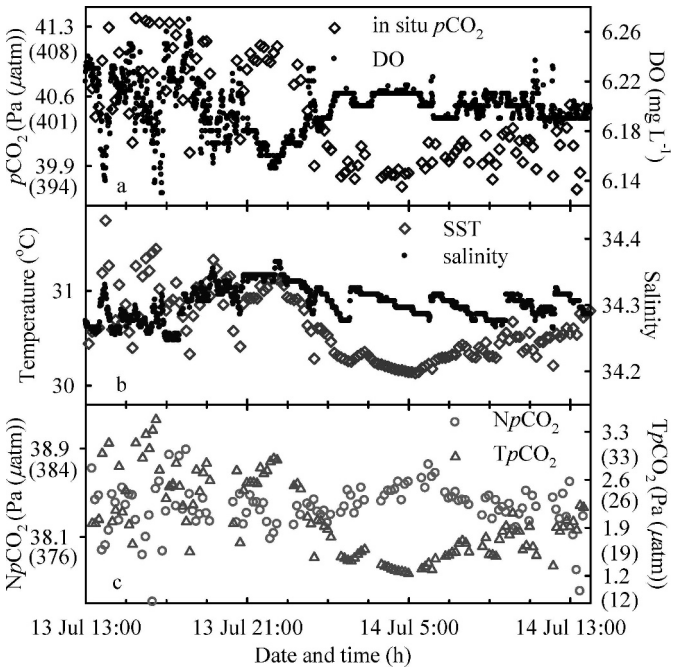

Fig. 3. Diurnal variations of surface seawater pCO_2, DO, temperature, and salinity at the basin of northern SCS (a, b). Also shown are the variations of temperature-normalized pCO_2 ($NpCO_2$) and $TpCO_2$ (pCO_2 offset caused by temperature variations, *see* text for details) (c). The figures were plotted by local time.

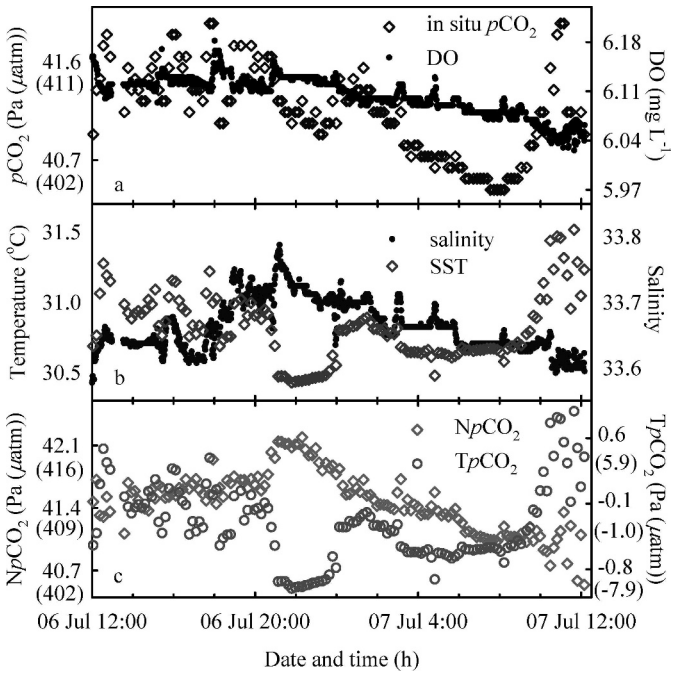

Fig. 4. Diurnal variations of surface seawater pCO_2, DO, temperature, and salinity at the Luzon Strait (a, b). Also shown are the variations of temperature-normalized pCO_2 ($NpCO_2$) and $TpCO_2$ (pCO_2 offset caused by temperature variations, *see* text for details) (c). The figures were plotted by local time.

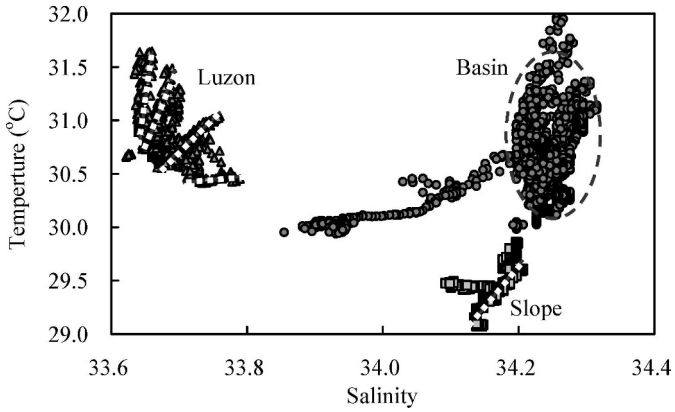

Fig. 5. Surface T – S diagrams at the stations on the slope, in the basin, and at Luzon Strait during the observation periods in this study.

similar with the regular semi-diurnal tide type in this region, the surface-water pCO_2 also showed a semi-diurnal pattern with peaks corresponding to low tides and lower values coinciding with high tides, exhibiting a good inverse correlation with the tidal height (Fig. 8). Similar to the Shenhu Bay station, in Xiamen Bay, pCO_2 also has a diurnal relationship with the tidal height which has a semi-diurnal tidal cycle (Fig. 9). But the pCO_2 variation did not show a clear pattern as in the Shenhu Bay. Nevertheless, based on all the data (the surface-water pCO_2 and tide height) there still appears an inverse correlation between pCO_2 and the tidal height.

Coral reef—The continuous observation conducted at Yongxing Island within a time frame of 18 d revealed that most of the observed biogeochemical parameters exhibited

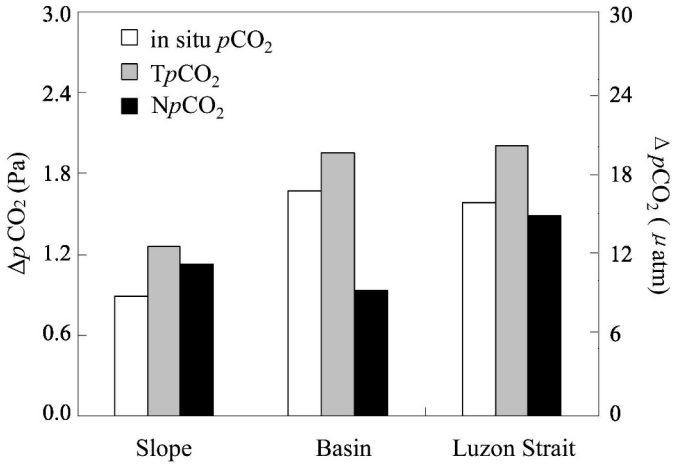

Fig. 6. Diurnal variation ranges of in situ pCO_2, T pCO_2, and N pCO_2 in surface seawaters at the oligotrophic sites under study in the northern South China Sea. ΔpCO_2 denotes the amplitude of pCO_2 change in one diurnal cycle. The white bar represents measured pCO_2 changes (in situ pCO_2), the grey bar represents the diurnal range of pCO_2 variation solely caused by temperature ($TpCO_2$), and the black bar represents the diurnal range of pCO_2 variation caused by nontemperature effects ($NpCO_2$).

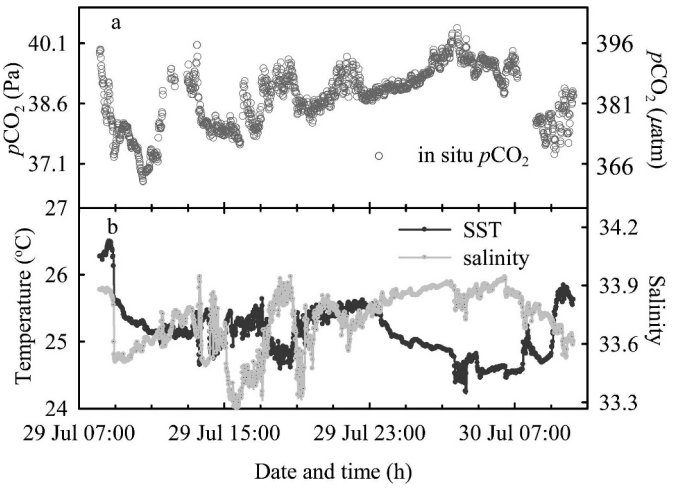

Fig. 7. Diurnal variations of surface seawater pCO_2, SST, and salinity at the station in the Taiwan Strait. The figures were plotted by local time.

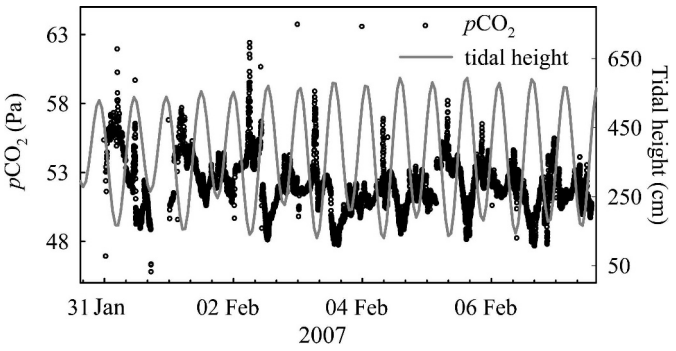

Fig. 9. Diurnal variations of surface seawater pCO_2 and tidal heights at the station in Xiamen Bay. The figures were plotted by local time. Note that the pCO_2 data shown in the figure were from a home-made pCO_2 sensor (*see* text for details) and have been reported in Lu et al. (2008).

significant periodic diurnal variations (Fig. 10). The surface seawater pCO_2 amplitudes in this system were as high as 20.3–60.8 Pa with a significant drawdown during the day and an increase during the night. DO consistently showed an inverse relationship with pCO_2, and also had a big variation range. Seawater temperature basically followed the diurnal cycle of solar radiation (not shown in the figure), and also had a negative correlation with pCO_2. Salinity does not show any clear cyclic trend of variation. The atmospheric pCO_2 during this period was ~38 Pa.

Discussion

Controls of the diurnal variations of surface seawater pCO_2—In an open system, aquatic pCO_2 is modulated by a variety of environmental conditions including temperature,

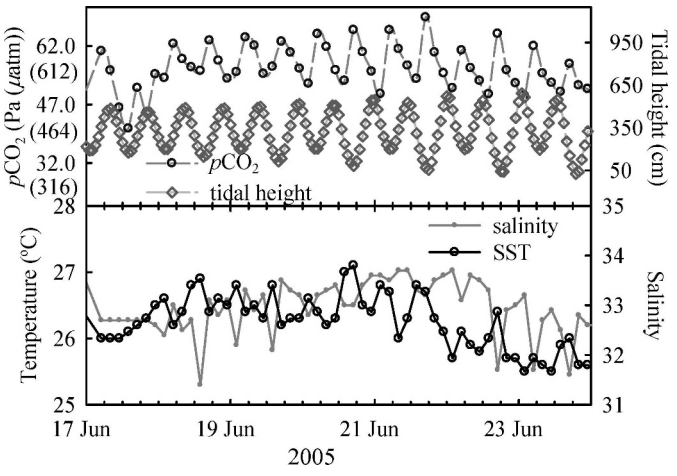

Fig. 8. Diurnal variations of surface seawater pCO_2, tidal height, SST, and salinity at the station in Shenhu Bay. The figures were plotted by local time. Note that the tidal height data are from Xiamen Bay, which is nearby. pCO_2 data shown in the figure were from a home-made pCO_2 sensor (*see* text for details) and have been reported in Lu et al. (2008).

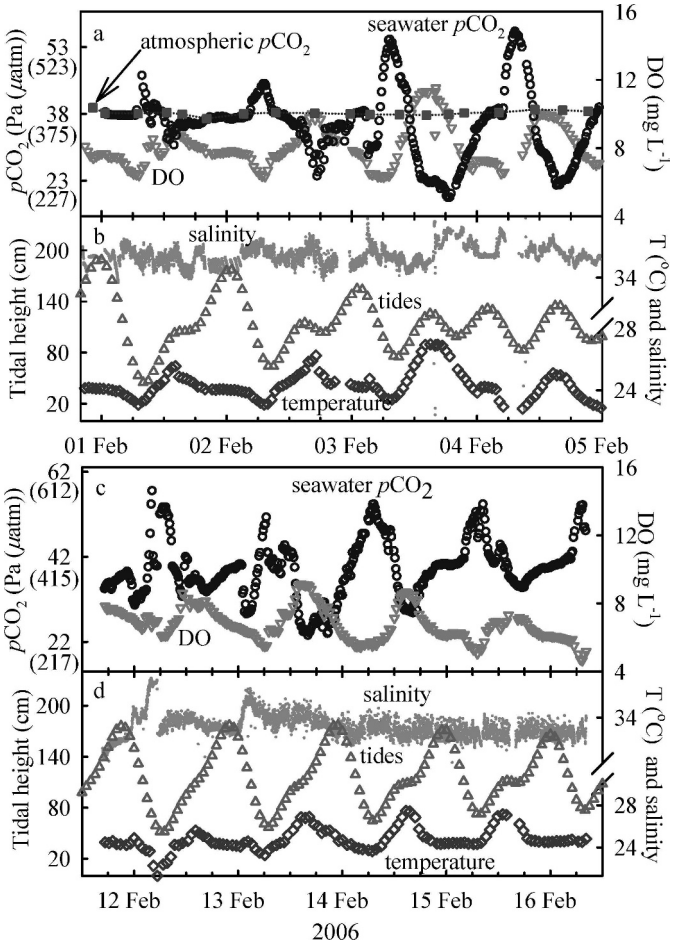

Fig. 10. Diurnal variations at Xisha Islands. All observations exhibited significant and regular diurnal variations, with seawater pCO_2 reaching its maximum (the pCO_2 can be as high as ~60.8 Pa) at 06 : 00–09 : 00 h and its minimum (the pCO_2 can be as low as ~20.3 Pa) at 17:00–19:00 h. The seawater pCO_2 takes on a distinct inverse correlation with DO and SST. However, there are no apparent correlations between seawater pCO_2 and salinity or tidal heights. The figures were plotted by local time.

current or tide, and biological activities. Temperature affects seawater pCO_2 through changing the thermodynamic conditions of the carbonate system, and current or tide determines seawater pCO_2 through mixing of different water masses. Biological metabolic processes may include photosynthesis, respiration, and calcium carbonate precipitation or dissolution, which alter the mass balance of the carbonate system and thus affect the pCO_2 in seawater. At all our experimental sites pCO_2 exhibited clear diurnal variations, the pattern of which was, however, different between sites, suggesting that different intrinsic processes may exist for controlling the diurnal variation.

Generally speaking, the surface seawater pCO_2 at our offshore sites was mainly controlled by temperature, while in nearshore areas, it seemed to be much more correlated with the tidal cycle and/or upwelling dynamics (i.e., the major control mechanism was the change of water masses). The pCO_2 in the coral reef system was the most dynamic case in all of our observations. The dominant control mechanisms were most likely photosynthesis and respiration. Calcium carbonate formation and dissolution regulated by corals and other microorganisms were also important. In this context and based upon our pCO_2 data and the other supporting parameters, we divided the controlling factors into three categories: temperature, tide or current, and biological activities.

Temperature control—The Pearson correlation coefficients between in situ pCO_2 and SST, salinity, and DO were 0.93, 0.14, and −0.38, respectively at the basin station, suggesting that SST was the major controlling factor. With a slightly different diurnal change pattern though, the pCO_2 at the Luzon Strait, also showed a good correlation with SST (the Pearson correlation coefficients between in situ pCO_2 and SST, salinity, and DO were 0.69, 0.18, and 0.25, respectively).

There did not appear to be strong evidence indicating that vertical or tidal mixing would contribute much to the pCO_2 variation at our offshore sites. The tidal ranges at the three sites are all small, <1 m (Table 1). Moreover, the slope and basin stations had a relatively stable and deep MLD (mixed-layer depth, average ~44 ± (5.7–8.6) m) during our observations (Table 2), and hence the change in vertical mixing would not significantly affect the sea surface pCO_2 in the course of the observation. The MLD at the Luzon Strait station, however, was much shallower and has even less variation (18 ± 1.6 m; Table 2). The limited changes in MLD at all three offshore sites would, therefore, suggest that the vertical mixing may not be a major factor affecting our observed diurnal variations of pCO_2.

In order to further examine how much temperature contributes to the change in surface seawater pCO_2, we subtracted N pCO_2 from in situ pCO_2, and obtained the pCO_2 offset caused by temperature variation (Fig. 3c), herein defined as T pCO_2 (T pCO_2 = in situ pCO_2 − N pCO_2). The temperature effect was on the order of 1.5–2.0 Pa at these three offshore sites. This result again supports the view that the variation of pCO_2 caused by the diurnal temperature cycle accounted mostly for in situ pCO_2 changes.

At the same time yet, the diurnal variation of pCO_2 upon normalization (i.e., N pCO_2 with a range of 38.0–38.8 Pa at the basin site [Fig. 3c]) still showed a pattern that appeared to be affected by biological metabolism during the diurnal cycle. For example, N pCO_2 dropped during daytime due to photosynthesis and increased during nighttime due to the respiration, showing a typical biological cycle driven by solar radiation (Fig. 3c). Unfortunately, the DO data fell between 6.16 mg L^{-1} and 6.24 mg L^{-1} with a variation only marginally higher than the precision of the YSI DO probe (~0.01 mg L^{-1}), which did not allow, therefore, for a quantitative evaluation of the biological effects. Nevertheless, the negative correlation between the in situ pCO_2 and N pCO_2 (Figs. 2c, 3c) suggested that the biological effect at these sites would be relatively minor.

It is not surprising that in the oligotrophic region of the SCS, the biological productivity is limited by its very low level of nutrients (Wu et al. 2003). Indeed, surface Chl *a* in this area was low (<0.12 μg L^{-1}). As a result, primary productivity and respiration were also reported to be relatively low (Cai et al. 2002; Liu et al. 2002). An observation near the basin station (115.5°E, 18.0°N) revealed a primary production of ~0.33 mmol C m^{-3} d^{-1} in the surface water (the corresponding DIN and Chl *a* were 0.1 μmol L^{-1} and 0.15 μg L^{-1}, respectively; Liu et al. 2002), similar to the average value of SCS in summer (Ning et al. 2004). As a first-order estimate, this 0.33 mmol C m^{-3} d^{-1} will result in a DIC change of 0.33 μmol L^{-1} at a daily timescale, equivalent to a pCO_2 change of merely 0.07 Pa assuming surface DIC ~1950 μmol kg^{-1}, pCO_2 ~40.5 Pa, and a Revelle factor of ~10.

By combining data from three oligotrophic sites, we further separated the temperature-dependent pCO_2 variation with those controlled by nontemperature factors (Fig. 6). Fig. 6 lent further evidence that the pCO_2 alteration by temperature (indicated by T pCO_2) was larger than the pCO_2 modulation by other factors (indicated by N pCO_2) at all three sites, although its relative importance of the temperature modulation differed.

Tide or current control—Coastal seas such as bays, straits and estuaries have complex hydrological conditions, and surface seawater pCO_2 in these localities may be significantly modulated by different water masses. Generally, ocean currents and tides are the two major forces bringing different water masses to a fixed station. Sometimes upwelling may also affect the surface seawater pCO_2 by introducing deep water with high pCO_2 to the surface through associated chemical and biological processes (Chen and Hsing 2005).

At the Taiwan Strait station, the Pearson correlation coefficients between in situ pCO_2 and salinity and temperature were 0.66 and −0.37, respectively, indicating high pCO_2 source water with high salinity and low temperature, possibly from upwelling of deeper offshore water. The reason why the correlation between pCO_2 and temperature was much weaker than that between pCO_2 and salinity was probably because salinity is more conservative

than temperature. The latter can be easily affected by solar radiation or evaporation. A multiple linear regression on the aforementioned three parameters provided Eq. 2.

$$pCO_2\ (\text{salinity,T}) = 27.607\ (\text{salinity}) - 2.632\ (\text{temperature}) - 482.586 \quad (2)$$

The coefficient for salinity was about one order of magnitude higher than that for temperature. Given the fact that these two parameters and their variation ranges were in a similar order of magnitude with a salinity range of 33.2–34.0 and a temperature range of 24.3–26.5°C, the much higher coefficient for salinity clearly indicated that salinity contributed much more to the pCO_2 change than temperature. This again suggested that different water masses are the major controlling factor for pCO_2 variation in this area.

In the diurnal observation experiment at the Shenhu Bay station, the inverse correlation between surface seawater pCO_2 and tidal height (Fig. 8) shows the tide control on pCO_2 as generally higher pCO_2 exists in nearshore water and lower pCO_2 exists in offshore water. Because the pCO_2 sensor deployed on the mooring only records data with a 3-h interval between each record, and the tidal phase has ~1 h of shift each day, we did not attempt to make a regression between surface-water pCO_2 and the tide height. In addition, we did not perform any calibration during the sensor's deployment because of mooring malfunction and the high sea condition. However, the lack of calibration would not affect the diurnal pattern or the above analysis.

The complex pattern of the surface-water pCO_2 at the Xiamen Bay station was also probably due to the fact that this station is near the city, the water mass was heavily influenced by river plume, sewage discharge, ship transport, and the like. However, the generic feature has still shown that pCO_2 was high during low tides and low during high tides (Fig. 9), suggesting that the influence of tides dominated the variation of pCO_2 again.

Biological control—As a highly productive open coral system of Xisha Islands, many factors may affect seawater pCO_2, and these are considered below in order to reveal the major controlling factor. Among other factors, photosynthesis and calcium carbonate dissolution may decrease pCO_2, whereas respiration and calcium carbonate production may increase seawater pCO_2 (Eqs. 3 and 4).

$$106CO_2 + 16HNO_3 + H_3PO_4 + 122H_2O \Leftrightarrow (CH_2O)_{106}(NH_3)_{16}H_3PO_4 + 138O_2 \quad (3)$$

$$Ca^{2+} + 2HCO_3^- \Leftrightarrow CaCO_3 + CO_2 + H_2O \quad (4)$$

In order to examine the temperature effect, we normalized seawater pCO_2 to a constant temperature by Eq. 1 according to Takahashi et al. (2002) and compared normalized seawater pCO_2 with in situ pCO_2. The result revealed that the temperature effect ranged from 0.1 Pa to 5.9 Pa with an average of only 2.4 Pa and, considering that the diurnal variation range was 20.3–60.8 Pa (or even higher) during this experiment, temperature cannot be a major factor controlling the pCO_2 diurnal variation. The inverse correlation between seawater pCO_2 and SST (Fig. 10) also demonstrated that although the solar radiation boosts photosynthesis and heats the seawater simultaneously, the effect of biological activities was far larger than the temperature effect on seawater pCO_2 in this coral reef system. The photosynthetic process apparently drew down the pCO_2 during the day but, at the same time, seawater temperature increased and raised pCO_2 slightly, and the amount of pCO_2 drawdown by photosynthesis was much greater than the pCO_2 rise due to temperature increase. At night, biological respiration increased pCO_2 persistently while decreasing seawater temperature because of heat loss and evaporation lowered pCO_2 only slightly.

Underway observations were also made outside the reef flat during three surveys in three different directions for as far as 10 nautical miles away from the Yongxingg Island, where the water depth was deeper than 1000 m. Surface seawater pCO_2 was generally equilibrated with the atmosphere with diurnal variations of no >1.0 Pa. As a result, water coming in with the tides generally diminished the amplitude of the diurnal variation observed on the reef. The average water depth of the reef flat around the Yongxing Island is ~10 m, with an irregular tide type of ~1 m. Ignoring the effects of currents other than tide, the daily exchange amount of the water mass inside the reef flat is ~10%. Consequently, tides are not the major factor controlling the pCO_2 diurnal variation. In addition, there was no clear correlation between the tidal height and the seawater pCO_2 as seen from their inconsistent changes between tidal cycles and between different observation periods (i.e., between Fig. 10a,b and Fig. 10c,d). This leaves biological activity as the only major controlling factor of the observed diurnal pCO_2 variation.

Surface seawater pCO_2 overall mirrored the DO variation (Fig. 10). Based on the fact that local consumption or production of oxygen is proportional to CO_2 production or utilization, and that the calcification or dissolution process does not alter DO, it was possible to separate the two processes responsible for CO_2 variations via analyzing the variation of DO. However, there are two insufficiencies of this method which may bring about considerable errors. First, the proportion between the biological production or utilization of O_2 and CO_2 is different from place to place (Chen et al. 1996). Second, the O_2 air–sea exchange rate is much faster than that of CO_2. We therefore used TA and DIC to constrain the biological uptake or release of inorganic carbon, and then to estimate the seawater pCO_2 alteration due to biological activities. Photosynthesis would deplete DIC and respiration would increase DIC as shown in Eq. 3. DIC, TA, and pCO_2 are also altered by calcification of coral reef organisms or dissolution as shown in Eq. 5. Thus, the amount of DIC consumption and production due to organic carbon production or decomposition should be corrected for alkalinity changes (Cai 2003). For precise calculation of small changes in TA due to organic matter production or decomposition, NO_3^- should be considered (Chen 1978; Chen et al. 1982), but its magnitude is negligible in coral reefs (Kinsey 1978). The extremely low DIN concentration

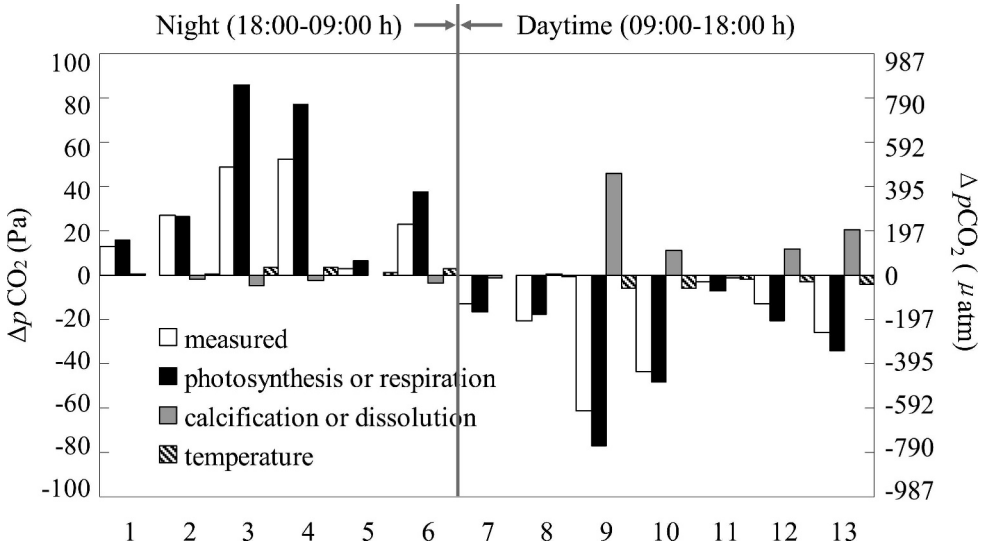

Fig. 11. Contributions to ΔpCO_2, the change in pCO_2 between a starting point and an end point in a monotonic decreasing or increasing segment by different controlling factors at the coral reef station at the Xisha Islands. The No. 1–13 represent 13 monotonic increasing and decreasing pCO_2 segments. The white bar represents measured pCO_2 changes in one segment, the black bar represents pCO_2 changes caused by photosynthesis or respiration, the grey bar represents pCO_2 changes due to TA variation, and the striped bar represents the temperature effects. The figure indicates that calcification and respiration have positive effects, and dissolution and photosynthesis have negative effects on pCO_2.

(<0.3 μmol L^{-1}) compared to the very high ΔDIC associated with photosynthesis or respiration also supported this view. Thus, we have

$$\text{DIC changes due to calcification or dissolution,} \quad \Delta DIC_{cal/diss} = \Delta TA/2 \tag{5}$$

$$\text{Biological DIC uptake or release,} \quad \Delta DIC_{oc} = \Delta DIC - \Delta TA/2 \tag{6}$$

To simplify the analysis, we arbitrarily divided each diurnal cycle into two segments: the monotonic decreasing pCO_2 segment from 09:00 h to 18:00 h, when the biological processes in seawater were generally dominated by photosynthesis; and the monotonic increasing pCO_2 segment from 18:00 h to 09:00 h the following day, when respiration prevailed. DIC generally decreased during the day because of the utilization of inorganic carbon in photosynthesis. TA also decreased due to net calcification of coral reef organisms. On the other hand, both DIC and TA increased at night due to respiration and dissolution of calcium carbonate. So, in a monotonic increasing or decreasing pCO_2 segment, the total changes of any parameter could be calculated by subtracting its starting-point value from its end-point value. Herein we use the subscript 0 to indicate starting-point and subscript 1 to indicate the end-point, and use ΔpCO_2 to indicate the pCO_2 difference between starting-point and end-point. In calculating pCO_2 alteration only due to photosynthesis or respiration, we have $\Delta TA = 0$, and $\Delta DIC = DIC_1 - DIC_0 - (TA_1 - TA_0) / 2$. However, in calculating pCO_2 change due to calcification or dissolution alone, we have $\Delta TA = TA_1 - TA_0$, and $\Delta DIC = DIC_0 + (TA_1 - TA_0) / 2$. All the DIC data were calculated from in situ TA and pH, and all carbonate system parameters were calculated using the "CO2SYS" program (Lewis and Wallace 1998). The result clearly demonstrated that photosynthesis and respiration accounted for the major changes of pCO_2 (Fig. 11). To further validate this calculation, we plotted the measured pCO_2 changes with the sum of pCO_2 changes caused by photosynthesis, calcification, and temperature (figure not shown) and this resulted in

$$\Delta pCO_2(\text{calculated}) = 1.1361 \times \Delta pCO_2(\text{measured}) + 83.234 \quad (R^2 = 0.9)$$

The calculated pCO_2 changes thus agreed very well with measured pCO_2 changes, suggesting that our calculations appeared to be in order.

Implication for the estimation of the air–sea CO_2 fluxes—Although we do not intend to extrapolate our diurnal observations to the open ocean, they do appear to have implications for estimates of air–sea CO_2 fluxes in the coastal ocean. Taking the SCS as an example, pCO_2 in the open area exhibits a diurnal variation of 1.0–1.6 Pa (assuming that these observed diurnal amplitudes were representative year-round), the CO_2 flux offset caused by this diurnal variation is $\pm$0.48–0.77 mmol C m^{-2} d^{-1} when compared with the median flux derived from the mean pCO_2 and the mean wind speed of $\sim$6.5 m s^{-1} obtained from three cruises that encompass three seasons in the northern SCS (Zhai et al. 2005). This offset is substantial

compared to the updated flux estimate of 0.4 mmol C m^{-2} d^{-1} for the northern SCS on an annual basis (Dai et al. unpubl.). On a global scale, Chen and Borges (in press) gave 3.0 mmol C^{-2} d^{-1} for the open areas of the marginal seas. Our estimate may, thus, account for 16–26% of the flux uncertainties for open areas in the marginal seas. Similarly, researchers found that short-term variability of pCO_2 (diurnal warming and cooling or atmospheric forcing) and frequency of sampling (every 3–4 d or monthly) affect estimates of net yearly CO_2 fluxes by >10–20% in the Sargasso Sea (Bates et al. 1998).

In the case of the continental shelf, our observed diurnal variations of 4.1 Pa (Fig. 7) could have caused an offset of ±1.76 mmol C m^{-2} d^{-1}. It should be noted that the air–sea CO_2 fluxes in the continental margin remain debatable, but that a current estimate is on the order of −1.9 mmol C m^{-2} d^{-1} (Cai et al. 2006). It must be pointed out that the continental shelf is a system characterized by highly variable distributions in space, and the value of 4.1 Pa in terms of daily changes may be regarded as a high value. When estuaries and bays are involved, diurnal variations can be dominant over seasonal or longer timescale changes. The amplitude of 5.1–15.2 Pa could cause an uncertainty of ±2.19–6.58 mmol C m^{-2} d^{-1}, again comparable to the current estimate of 24.8 mmol C m^{-2} d^{-1} as a global scale estimate (Borges et al. 2005). However, we should point out that the regions where the diurnal cycle is large probably have small surface areas relative to the typically more oligotrophic coastal ocean as revealed in this study. It is also worth pointing out that uncertainties in the estimate of CO_2 fluxes from the coastal ocean may also come from the gas-transfer velocity. We used in this study the Wanninkhof (1992) equation to estimate the gas-transfer velocity, which is, however, believed to be site-specific, especially in coastal environments where currents play a major role (Borges et al. 2004).

Though they occupy only 0.2% of the global ocean area, coral reefs have one of the highest primary production rates among natural ecosystems, and the two major processes of reef systems are organic carbon metabolism (photosynthesis and respiration) and the inorganic carbon metabolism (calcification and dissolution of calcium carbonate). Taking the reef system of Xisha Islands as an example, it was dominated mainly by biological activities, and the surface seawater pCO_2 there varied throughout the day, generally reaching its lowest value (as low as <15.2 Pa) in the afternoon and highest value (as high as >91.2 Pa) in the early morning. The corresponding magnitude of sink and source is −15.1 (air to sea) mmol C m^{-2} d^{-1} and +41.2 mmol C m^{-2} d^{-1} (sea to air), respectively, using the mean wind speed of ~5.3 m s^{-1} measured at a meteorological station. If averaging all the diurnal amplitudes of seawater pCO_2 over the study period, it still has an average diurnal variation from 29.2 Pa to 60.8 Pa, which corresponds to an air–sea flux of −6.0–15.3 mmol C m^{-2} d^{-1}. By integrating all the time-series pCO_2 data, the studied area is a weak source of atmospheric CO_2 at ~1.48 mmol C m^{-2} d^{-1}.

Most air–sea CO_2 flux studies have been conducted on shipboard cruises. This approach is favorable in flux estimation in a large and relatively homogeneous region, if the cruise covers at least one diurnal cycle for the specific region. However, in some coastal seas like bays, estuaries, and reef systems, where tidal cycles and surface seawater pCO_2 diurnal variability are significant, underway measurement may show potential bias in its temporal representation of a particular study area, causing some error if, for example, measurements were conducted during daytime; the estimated flux error could exceed the flux itself. Adding more complexity is the fact that the diurnal variability may be subject to latitudinal differences (e.g., higher biological effects at higher latitudes) making the estimate even more difficult to constrain. We contend that underway measurements alone are inherently not sufficient to resolve the diurnal, seasonal, and inter-annual pCO_2 variations in surface seawater, and diurnal variability may result in a larger uncertainty in estimating air–sea CO_2 flux in nearshore settings if proper timescale of averaging is not considered.

Acknowledgments

We are grateful to the Shandong Institute of Oceanographic Instrumentation, Xiamen Marine Environment Monitoring Station, and Xisha Marine Environment Monitoring Station of State Oceanic Administration for providing facilities and logistic support. The crews of R/V *Yanping II* and *Dongfanghong II* provided much help during the sampling campaigns. Comments and suggestions from two anonymous reviewers and Jack J. Middelburg have greatly improved the quality of the paper. John Hodgkiss is thanked for his editorial help with English. We acknowledge financial support by the National Science Foundation of China through grants 90211002, 40490264, 40521003.

References

Bates, N. R., L. Samuels, and L. Merlivat. 2001. Biogeochemical and physical factors influencing seawater fCO_2, and air–sea CO_2 exchange on the Bermuda coral reef. Limnol. Oceanogr. **46:** 833–846.

———, T. Takahashi, D. W. Chipman, and A. H. Knap. 1998. Variability of pCO_2 on diel to seasonal timescales in the Sargasso Sea near Bermuda. J. Geophys. Res.-Oceans **103:** 15567–15585.

Borges, A. V., B. Delille, and M. Frankignoulle. 2005. Budgeting sinks and sources of CO_2 in the coastal ocean: Diversity of ecosystems counts. Geophys. Res. Lett. **32:** L14601, doi:10.1029/2005GL023053.

———, ———, L. S. Schiettecatte, F. Gazeau, G. Abril, and M. Frankignoulle. 2004. Gas transfer velocities of CO_2 in three European estuaries (Randers Fjord, Scheldt and Thames). Limnol. Oceanogr. **49:** 1630–1641.

———, and M. Frankignoulle. 1999. Daily and seasonal variations of the partial pressure of CO_2 in surface seawater along Belgian and southern Dutch coastal areas. J. Mar. Syst. **19:** 251–266.

Cai, P. H., Y. P. Huang, M. Chen, L. D. Guo, G. S. Liu, and Y. S. Qiu. 2002. New production based on Ra-228-derived nutrient budgets and thorium-estimated POC export at the intercalibration station in the South China Sea. Deep-Sea Res. I **49:** 53–66.

Cai, W. J. 2003. Riverine inorganic carbon flux and rate of biological uptake in the Mississippi River plume. Geophys. Res. Lett. **30:** 1032–1036, doi:10.1029/2002GL016312.

———, and M. Dai. 2004. Comment on "Enhanced open ocean storage of CO_2 from shelf sea pumping". Science **306:** 1477.

———, ———, AND Y. C. WANG. 2006. Air–sea exchange of carbon dioxide in ocean margins: A province-based synthesis. Geophys. Res. Lett. **33:** L12603, doi:10.1029/2006GL026219.

———, AND OTHERS. 2004. The biogeochemistry of inorganic carbon and nutrients in the Pearl River estuary and the adjacent Northern South China Sea. Cont. Shelf Res. **24:** 1301–1319.

CHEN, C. T. A. 1978. Decomposition of calcium-carbonate and organic-carbon in deep oceans. Science **201:** 735–736.

———. 2003. Rare northward flow in the Taiwan Strait in winter: A note. Cont. Shelf Res. **23:** 387–391.

———, AND A. V. BORGES. In press. Reconciling opposing views on carbon cycling in the coastal ocean? Continental shelves as sinks and nearshore ecosystem as sources of atmospheric CO_2. Deep-Sea Res. II. doi:10.1016/j.dsr2.2009.01.001.

———, AND L. Y. HSING. 2005. Degree of nutrient consumption as an aging index of upwelling or vertically mixed water in the northern Taiwan Strait. Acta Oceanol. Sin. **24:** 115–124.

———, C. M. LIN, B. T. HUANG, AND L. F. CHANG. 1996. Stoichiometry of carbon, hydrogen, nitrogen, sulfur and oxygen in the particulate matter of the western North Pacific marginal seas. Mar. Chem. **54:** 179–190.

———, R. M. PYTKOWICZ, AND E. J. OLSON. 1982. Evaluation of the calcium problem in the South-Pacific. Geochem. J. **16:** 1–10.

CHEN, Y. L. L., AND H. Y. CHEN. 2006. Seasonal dynamics of primary and new production in the northern South China Sea: The significance of river discharge and nutrient advection. Deep-Sea Res. I **53:** 971–986.

———, ———, AND Y. H. LIN. 2003. Distribution and downward flux of Trichodesmium in the South China Sea as influenced by the transport from the Kuroshio Current. Mar. Ecol.-Prog. Ser. **259:** 47–57.

DEGRANDPRE, M. D., R. WANNINKHOF, W. R. MCGILLIS, AND P. G. STRUTTON. 2004. A Lagrangian study of surface pCO_2 dynamics in the eastern equatorial Pacific Ocean. J. Geophys. Res.-Oceans **109:** C08S07, doi:10.1029/2003JC002089.

DICKEY, T. D. 2004. Exploration of biogeochemical temporal variability, p. 149–188. *In* M. Follows and T. Oguz [eds.], The ocean carbon cycle and climate. NATO Advanced Study Inst. Ser. Kluwer Academic.

———, AND R. R. BIDIGARE. 2005. Interdisciplinary oceanographic observations: The wave of the future Sci. Mar. **69:** 23–42.

FRANSSON, A., M. CHIERICI, AND L. G. ANDERSON. 2004. Diurnal variability in the oceanic carbon dioxide system and oxygen in the Southern Ocean surface water. Deep-Sea Res. II **51:** 2827–2839.

GUO, W., X. ZHANG, Y. YANG, AND M. HU. 1998. Potential eutrophication assessment for Chinese coastal waters. J. Oceanogr. Taiwan Strait **17:** 64–70 [In Chinese.].

JAN, S., J. WANG, C. S. CHERN, AND S. Y. CHAO. 2002. Seasonal variation of the circulation in the Taiwan Strait. J. Mar. Syst. **35:** 249–268.

KINKADE, C. S., J. MARRA, T. D. DICKEY, C. LANGDON, D. E. SIGURDSON, AND R. WELLER. 1999. Diel bio-optical variability in the Arabian Sea as observed from moored sensors. Deep-Sea Res. II **46:** 1813–1832.

KINSEY, D. W. 1978. Alkalinity changes and coral-reef calcification. Limnol. Oceanogr. **23:** 989–991.

KUSS, J., W. ROEDER, K. P. WLOST, AND M. D. DEGRANDPRE. 2006. Time-series of surface water CO_2 and oxygen measurements on a platform in the central Arkona Sea (Baltic Sea): Seasonality of uptake and release. Mar. Chem. **101:** 220–232.

LEWIS, E., AND D. W. R. WALLACE. 1998. Program developed for CO_2 system calculations. Oak Ridge Natl. Lab., Carbon Dioxide Info. Anal. Cent., ORNL/CDIAC-105. U.S. Dept. of Energy.

LIU, K. K., S. Y. CHAO, P. T. SHAW, G. C. GONG, C. C. CHEN, AND T. Y. TANG. 2002. Monsoon-forced chlorophyll distribution and primary production in the South China Sea: Observations and a numerical study. Deep-Sea Res. I **49:** 1387–1412.

LU, Z., M. DAI, K. XU, J. CHEN, AND Y. LIAO. 2008. A high precision, fast response, and low power consumption in situ optical fiber chemical pCO_2 sensor. Talanta **76:** 353–359, doi:10.1016/j.talanta.2008.03.005.

LUO, D. 2002. Study on the distribution of dissolved oxygen in Shenhu Bay and its relationship with phytoplankton and suspended matter. Mar. Sci. Bull. **21:** 31–36. [In Chinese.].

MARRA, J. 1997. Analysis of diel variability in chlorophyll fluorescence. J. Mar. Res. **55:** 767–784.

MONTEGUT, C. D., G. MADEC, A. S. FISCHER, A. LAZAR, AND D. IUDICONE. 2004. Mixed layer depth over the global ocean: An examination of profile data and a profile-based climatology. J. Geophys. Res.-Oceans **109:** doi:10.1029/2004JC002378.

NIE, B., T. CHEN, M. LIANG, Y. WANG, J. ZHONG, AND Y. ZHU. 1996. The relationship between coral growth rate at Northern SCS and sea surface temperature during the past 100 years. Sci. China Ser. D Earth Sci. **26:** 59–66. [In Chinese.].

NING, X., F. CHAI, H. XUE, Y. CAI, C. LIU, AND J. SHI. 2004. Physical–biological oceanographic coupling influencing phytoplankton and primary production in the South China Sea. J. Geophys. Res.-Oceans **109:** C10005, doi:10.1029/2004JC002365.

RUAN, J. 2001. Distribution and characteristics of chlorophyll-*a* content at spring and autumn in Shenhu Bay. J. Fujian Fish. **88:** 1–7. [In Chinese.].

TAKAHASHI, T., AND OTHERS. 2002. Global sea–air CO_2 flux based on climatological surface ocean pCO_2, and seasonal biological and temperature effects. Deep-Sea Res. II **49:** 1601–1622.

WANNINKHOF, R. 1992. Relationship between wind-speed and gas-exchange over the ocean. J. Geophys. Res.-Oceans **97:** 7373–7382.

WEISS, R. F. 1974. Carbon dioxide in water and seawater: The solubility of a non-ideal gas. Mar. Chem. **2:** 203–215.

WU, J. F., S. W. CHUNG, L. S. WEN, K. K. LIU, Y. L. L. CHEN, H. Y. CHEN, AND D. M. KARL. 2003. Dissolved inorganic phosphorus, dissolved iron, and *Trichodesmium* in the oligotrophic South China Sea. Glob. Biogeochem. Cycles **17:** 1008, doi:10.1029/2002GB001924.

YATES, K. K., C. DUFORE, N. SMILEY, C. JACKSON, AND R. B. HALLEY. 2007. Diurnal variation of oxygen and carbonate system parameters in Tampa Bay and Florida Bay. Mar. Chem. **104:** 110–124.

YUAN, D. L., W. Q. HAN, AND D. X. HU. 2006. Surface Kuroshio path in the Luzon Strait area derived from satellite remote sensing data. J. Geophys. Res.-Oceans **111:** C11007, doi:10.1029/2005JC003412.

ZHAI, W. D., M. H. DAI, W. J. CAI, Y. C. WANG, AND H. S. HONG. 2005. The partial pressure of carbon dioxide and air–sea fluxes in the northern South China Sea in spring, summer and autumn. Mar. Chem. **96:** 87–97.

Associate editor: Jack J. Middelburg

Received: 19 July 2008
Accepted: 26 November 2008
Amended: 15 January 2009